



Prediction of reconnaissance drought index and standardized precipitation index for drought analysis



Zahraa M. Kadhum^{a,b*}, Amjad N. Mohsin Alhameedawi^b, Mustafa N. Hamoodi^b

^a Technical Institute of Babylon, Al-Furati Al-Awsat Technical University, Babylon, Iraq.

^b Civil Engineering Dept., University of Technology-Iraq, Alsina'a street, 10066 Baghdad, Iraq.

*Corresponding author Email: zahraa.musa@atu.edu.iq

HIGHLIGHTS

- Drin C was used to analyze drought using the Reconnaissance Drought Index (RDI) and Standard Precipitation Index (SPI).
- A hybrid model was proposed to improve drought prediction accuracy over traditional linear and nonlinear methods.
- Drought duration, intensity, and accumulative deficit were evaluated for each station.
- ARIMA improved SPI and RDI prediction, reaching R^2 values of 0.95 for SPI12 and 0.818 for RDI12.

Keywords:

ARIMA model
Drin C software
Standard precipitation index
Random forest

ABSTRACT

Drought is a natural disaster characterized by its intensity, duration, and spatial extent. This research investigates meteorological drought in Babylon Province, Iraq, highlighting its significance in the local context, particularly given the region's vulnerability to climatic changes. Employing the Drought Index Calculator (Drin C), we evaluate drought indices, namely the Reconnaissance Drought Index (RDI) and the Standard Precipitation Index (SPI), from 1991 to 2021. This study underscores the imperative of assessing the accuracy of commonly used drought monitoring techniques due to their inherent uncertainties. This work highlights the importance of integrating advanced modelling tools, such as the integration of advanced modeling tools, such as Random Forest and ARIMA, alongside comprehensive meteorological assessments to enhance drought preparedness and response strategies. The project aims to deepen the understanding of drought conditions in Babylon Province by employing sophisticated analytical models and evaluating their efficacy in forecasting drought indicators, while providing data-driven recommendations for efficient water resource management. The model utilizes monthly precipitation data from six sites to calculate SPI and RDI values, with R-squared values of 0.95 for SPI12 and 0.818 for RDI12, clearly attributing these values to the ARIMA model. The ARIMA model enhances predictive accuracy with increasing time scales, while the Random Forest model offers complementary insights into drought patterns. A hybrid model for drought forecasting is created, combining linear and nonlinear approaches, which progressively enhances precision and provides significant insights into local climate variability, thereby facilitating effective decision-making and resource management.

1. Introduction

Drought is a significant natural disaster characterized by an extended reduction in rainfall, leading to water scarcity and severe environmental, economic, and agricultural impacts [1-3]. This phenomenon is increasingly exacerbated by climate change, resulting in a rise in the severity and frequency of drought events, particularly in vulnerable regions like Iraq and Babylon Province. Evaluating drought severity within this hydrological context, while considering temporal and spatial aspects, is essential for efficient planning and management of water resources [4,5]. The challenges of accurately assessing drought in Iraq include limited historical data, varying regional climate patterns, and socio-economic factors that complicate response strategies. [6-8]. Drought can be broadly classified into four types: meteorological, hydrological, agricultural, and socioeconomic [9-11]. Drought indices are crucial for predicting and mitigating drought effects. They help meteorological and hydrological stations predict drought events using relevant climatic data. Studies widely use drought indices like the Standardized Precipitation Index (SPI) and Reconnaissance Drought Index (RDI) to monitor and forecast droughts in various areas [12]. The RDI was used to determine the temporal and spatial analysis of meteorological drought in Iraq [13,14].

Similarly, numerous research investigations have advocated the RDI as a climatic index for identifying potential climate changes. Drought indicators are generally continuous functions of temperature, rainfall, river discharge, or other measurable hydro-meteorological factors. One of the most commonly used drought indices is the Standardized Precipitation Index (SPI) [15,16]. Drought analysis was done in the Meric-Ergene, Gediz, Seyhan, and Ceyhan river basins in Turkey using SPIs and monthly rainfall information [17,18]. Poshard's and Michaelides investigated regional drought assessment by computing the SPI and RDI indices, which rely on historical monthly rainfall and temperature data. We can effectively use the two indices to assess and observe drought conditions and occurrences [19,20]. In Iran, a separate study utilizes the SPI and RDI indices over several time frames at forty meteorological sites. Linear regression models are constructed based on linear relationships between dependent and independent variables [21,22].

The method relies on a drought index as a dependent variable, with precipitation and temperature as independent factors, but its linearity becomes questionable in complex investigations. ARIMA is a prevalent statistical technique for time series analysis and forecasting, effectively capturing diverse temporal features within data [23,24].

Seasonal Autoregressive Integrated Moving Average (SARIMA) and Autoregressive Integrated Moving Average (ARIMA) are used to address this drawback [25,2] Mossad and Alazba, developed ARIMA models for drought forecasting in hyperarid climates, showing potential for different time scales. Stochastic models struggle with nonlinear data, leading researchers to use artificial neural networks for hydrological prediction increasingly [26,27]. Support Vector Regression (SVR) model and its enhanced variants, fuzzy-SVR, are used by Fung et al. (2020), to predict the SPEI with a 1-month lead time. The F-SVR model improved accuracy with increasing SPEI time scales. On the other hand, other models were discussed for meteorological drought predictions downstream of the Langat River basin [28-30]. ARIMA models are crucial for time series analysis in economics, environmental science, and agriculture, accurately forecasting climatic phenomena like drought in Iraq and aiding farmers in water resource management [31,32].

Iraq is a country in the Middle East that has experienced frequent drought occurrences in recent decades. This significantly impacted water resources, irrigated and rainfed agriculture, cultivated land areas, desertification, and demographic distribution, hence resulting in substantial economic challenges for the country. For example, between 2000 and 2020, Iraq experienced drought conditions in approximately 10 out of 20 years, with more than 30% of its agricultural land affected, exacerbating problems such as desertification and resource scarcity [33,34]. This study intends to investigate and assess meteorological drought in Babylon Province. Standardized Precipitation Index (SPI) and Reconnaissance Drought Index (RDI). The ARIMA model was employed as a temporal model based on a drought index time series to analysis drought event characteristics, including the steady-state probability of drought occurrences, the mean duration of droughts, and drought susceptibility.

The objectives of this paper are to assess meteorological drought using the Standardized Precipitation Index (SPI) and the Reconnaissance Drought Index (RDI). It also aims to analyze drought conditions in Babylon Province using these indices. In addition, it seeks to compare the effectiveness of SPI and RDI in evaluating drought conditions.

2. Materials and methods

2.1 Study area

The research focuses on the Babylon Province in Iraq, covering 5.338 Km². Babylon Province is located between 44°2'43" E and 45°12'11" E and 32°5'41" N and 33°7'36" N, as shown in Figure 1. The region has an arid climate with high temperatures, drought, and scarce rainfall. Surrounded by the Euphrates River, it experiences extreme heat and dry weather. The city has evolved into a technological center, offering opportunities for economic expansion and industrial advancement [35,36]. However, the region experiences significant temperature variations.

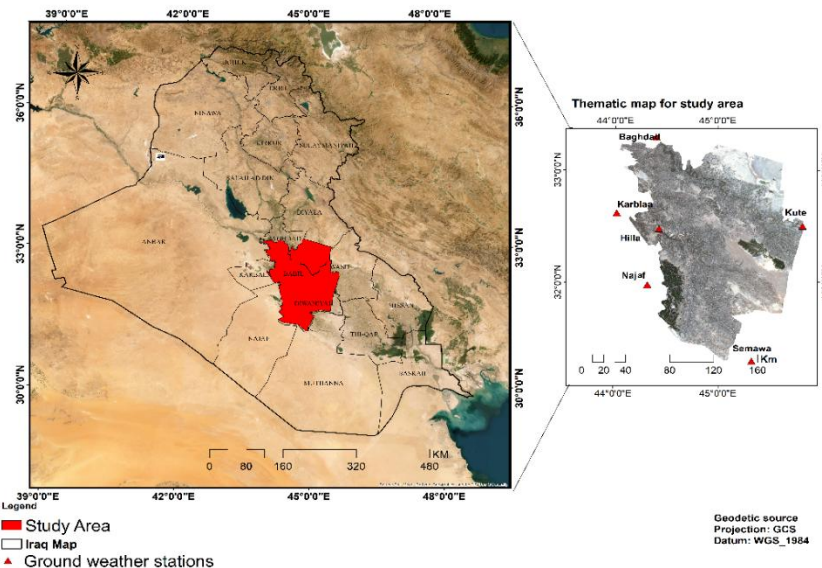


Figure 1: Geographical location maps the study area (by researcher)

2.2 Data acquisition

The meteorological data required for the study were collected from the General Authority of Meteorology and Seismic Monitoring (GMSM). The information includes the maximum and minimum temperature, precipitation, and daily streamflow data of 20 years from 1991 to 2021, respectively. The data required for the study were collected from the metrological station as illustrated in Table 1.

Table 1: Meteorological Stations around the study area for the period 1991-2021

No.	Station name	Easting	Northing	Elevation	Tmin (°C)	Tmax (°C)
1	Baghdad	44°21'58"	54° 33' 18"	32.0	16.0	31.3
2	Karbala	44° 0' 32"	32° 36' 4"	34.6	18.3	31.6
3	Hilla	44° 25' 36"	32° 28' 31"	33.0	16.8	31.5
4	Najaf	44° 30' 18"	32° 0' 18"	46.4	18.5	32.1

2.3 Software used

2.3.1 Drin C

Drin C (Drought Indices Calculator) is a specialized tool for drought indices analysis. The program includes several well-known drought indices, such as the Precipitation-based Drought Index (SPI), Reconnaissance Drought Index (RDI), Streamline Drought Index (SDI), and Decadal Precipitation Index (PD). On the other hand, there is the option to use both approaches for each index, which also allows the comparison of the results between RDI and SPI. Furthermore, the use of gamma or lognormal distributions is supported. Drin C possesses comprehensive graphical user interface (GUI) capabilities and operates on Microsoft Windows operating systems. During the software package development, focus was placed on keeping a basic, comprehensive, and user-friendly structure. The indexes aim to provide clear results for efficient operational use and minimize data requirements, distributions that may be selected [37].

2.3.2 Orange

Orange is a component-based visual programming software suite for data analysis and machine learning. From basic data visualisation, subset selection, and preprocessing to empirical assessment of learning algorithms and predictive modelling [38]. Time series data was examined using Orange software, which also used the ARIMA model to forecast drought index values for the next ten years. The study used the drought indicators SPI and RDI to evaluate the severity of drought in the examined region. Over several years, monthly rainfall data were gathered, and the SPI and RDI values were computed from it. The data was handled by Orange software, which also converted the time series into a suitable format for the ARIMA model and managed missing values. Data analysis led to the selection of the appropriate model. After estimating the model, metrics like RMSE were used to evaluate the accuracy of the predictions, and future values were forecasted using the model to predict SPI and RDI index values for the upcoming decade, which aided in understanding potential drought patterns. Data analysis led to the selection of the appropriate model. After estimating the model, metrics like RMSE were used to evaluate its accuracy. Then, future values were forecasted by using the model to predict SPI and RDI index values for the upcoming decade, which aided in understanding potential drought patterns.

2.4 Drought indices overview

The drought indices are provided below, along with a brief description that supports the severity of the drought. The selection of these indices was driven by two primary goals: (a) having a minimal data requirement, which would allow the program to be applied in multiple regions, and (b) having results that are easy to understand and use effectively in the field. The Reconnaissance Drought Index (RDI) and the Standardized Precipitation Index (SPI) were incorporated into the Drin C according to these standards. For interpreting SPI and RDI, it's easiest to look at the meteorological drought that occurred when precipitation was the primary variable (and, for RDI only, possible evapotranspiration) [39].

2.4.1 Standard precipitation index (SPI)

At Colorado State University, McKee et al. [16], created the SPI in 1992. His work was initially showcased during the Eighth Congress of Applied in January 1993. The weather was used to determine the SPI, and the long-term precipitation record for the given time frame was transformed from a probability distribution into a standard distribution. This process ensures that the mean SPI for the given circumstance and desired time frame is zero [16,40]. A lower SPI value indicates less precipitation than the median, while a higher value suggests more precipitation than the median. The normalization of SPI allows for equal representation of drier and wetter climates. The most significant benefit of the SPI is its ability to be easily used and calculated through the use of precipitation data [41]. Equations (1, 2 and 3) were used to compute SPI:

$$SPI = S \frac{t - (c_2 t + c_1) + c_0}{[(d_3 t + d_2) t + d_1] t + 1} \quad (1)$$

$$t = \ln \frac{\sqrt{1}}{G(x^2)} \quad (2)$$

$G(x^2)$ is the probability distribution of rainfall associated with the gamma (G) function; x is the precipitation sample value; S is the probability density positive and negative coefficient; and C_0 , C_1 , and C_2 and d_1 , d_2 , and d_3 are the calculation parameters for the G distribution function to convert to the cumulative frequency simplified approximate solution formula as Equation (3):

$$G(X) = \frac{2}{\beta\gamma\Gamma(\gamma)} \int_0^x x^{\gamma-1} e^{-x/\beta} dx, x > 0 \quad (3)$$

where γ is the shape parameter and β is the scale parameter of the Γ distribution function.

Table 2 presents the classification of dry and wet spells based on SPI values.

Table 2: Categorization of Drought Conditions Based on the (SPI)

SPI values	Classification
2.0 or more	Extremely wet
1.5 to 1.99	Very wet
1.0 to 1.49	Moderately wet
-0.99 to 0.99	Near normal
-1.0 to -1.49	Moderately dry
-1.5 to -1.99	Severely dry
-2.0 or less	Extremely dry

2.4.2 Reconnaissance drought index (RDI)

The Reconnaissance Drought Index (RDI) was created to assess water shortage more accurately, serving as a balance between input and production within a water system. RDI is based on both cumulative precipitation (P) and potential evapotranspiration (PET), which is one measured (P) and the other one calculated (PET) determinant [42,18]. The value (αk) of RDI is calculated for the i -th year on the basis of the time of k (months) as in Equations (4) and (5) as follows:

$$\alpha k^i = \frac{\sum_{j=1}^k p(i,j)}{\sum_{j=1}^k PET_{ij}}, i = 1(1)N^j = 1(1)k \quad (4)$$

The Equation for calculating RD_{1st}, where P_{ij} and PET_{ij} represent precipitation and potential evapotranspiration in the j -th month of the i -th year, and N is the total number of years of available data, follows both lognormal and gamma distributions across various locations and time scales. The intensity ratings presented in Table 3 can be utilised to categorise drought [43].

$$RD_{1st}^i = \frac{y^i - y}{\hat{\sigma}y} \quad (5)$$

Table 3: Classification of drought conditions according to the RDI

State	Description	Criterion
01	mild	-0.5 to -1.0
02	moderate	-1.0 to -1.5
03	severe	-1.5 to -2.0
04	extreme	< -2.0

$y(i)$ is the natural logarithm of αk (i), y is the arithmetic mean, and $b \sigma y$ signifies its standard deviation. When employing the gamma distribution, the RD_{1st} can be ascertained by fitting the gamma probability density function (pdf) to the designated frequency distribution of αk . Positive RD_{1st} values indicate wet periods, while negative values represent dry periods, in contrast to the realm's typical conditions [42,44].

2.5 ARIMA model

One common tool in hydrometeorological research is the ARIMA (Autoregressive Integrated Moving Average) model, which is especially useful when studying extreme weather events like droughts [45,46]. Assuming the time series data is stationary is a key component of a successful application; this may call for treatments like differencing or logarithmic adjustments. Choosing the right sequence of patterns of variation is crucial, and the Autocorrelation and Partial Autocorrelation Functions (ACF and PACF) might help with that [46]. Additionally, the model's goodness of fit is evaluated using statistical metrics such as the Akaike Information Criterion (AIC) and the Bayesian Information Criterion (BIC), where lower values indicate a better fit [47,48]. The research assesses the efficacy of a novel drought prediction system employing SPI-12 and RD₁₂, using MSE and R². It presents an ARIMA model, combining linear ARIMA and nonlinear SVR models, for 1-12 months, enhancing accuracy and explanatory power. The ARIMA model forecast flowchart is shown in Figure 2. The ARIMA model is given by Equation 6.

$$\phi(B)(1 - B^d)y_t = \theta(B)\varepsilon_t \quad (6)$$

where B = the shift function., $\phi(B)$ = Autoregressive (AR) function, describing the impact of preceding values of the time series on the present value, $\theta(B)$ = Moving Average (MA) function, which defines the influence of historical errors, ε_T = Error period at time t .

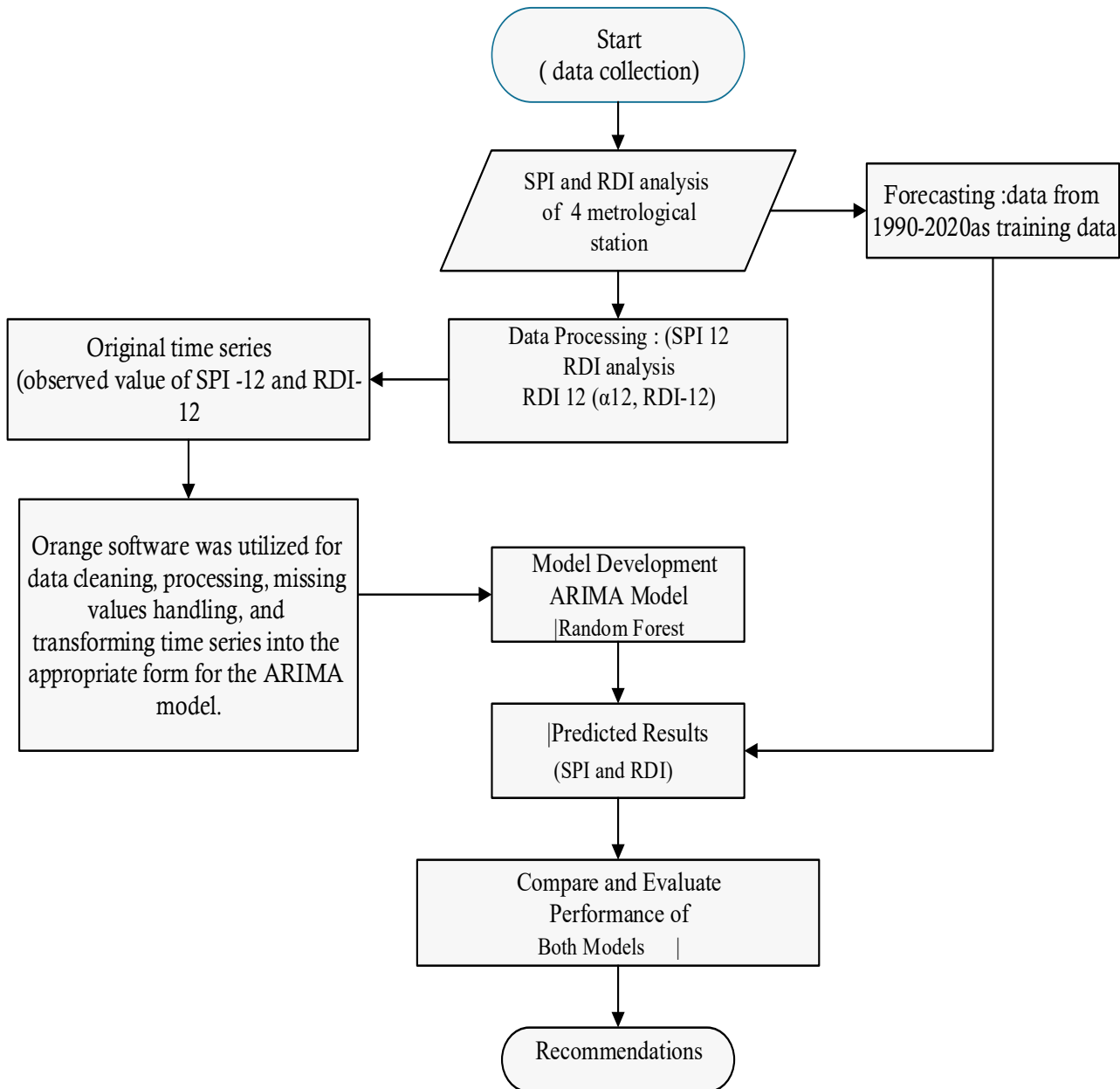


Figure 2: Methodology of the ARIMA and (RF) Model for Forecasting

2.6 Random forest model

Leo Breiman's random forest (RF) technique is now a de facto method for bioinformatics data analysis. It manages complex interaction structures and highly correlated variables with ease and returns measures of variable relevance; it also performs admirably in situations when the number of variables is significantly higher than the number of observations. The study predicts RDI and SPI using Leo Breiman's random forest algorithm, a machine learning technology known for its excellent prediction accuracy and straightforward training procedure. In our study, we utilized a specific number of trees set to [500] as in Equation (7), to ensure robust performance. Additionally, the hyperparameters were adjusted using [grid search], which allowed us to optimize model accuracy. Breiman et al. [49], developed the RF ensemble algorithm in 2001. It is based on decision trees and predictors [49].

$$\hat{y} = \frac{1}{N} \sum_{i=1}^N T_i (X) \quad (7)$$

where N is the number of trees in the forest, $T_i(X)$ is the prediction made by the i -th tree for the input features X .

2.7 Assessment of the validity index

To assess the model's accuracy in predicting the observed values, this study employed RMSE, MAE, R², and NSE (Nash 1970). RMSE The method determines the value that is most distant from the actual value. The model's performance is rated by its prediction error, with a lower RMSE indicating better generalization to unseen data compared to its fit on training data [50].

Mean absolute error (MAE) is a more accurate measure of the anticipated value error that can more accurately reflect the real situation. Regression models use the mean value as a baseline for the error, employing R² to evaluate whether the prediction error exceeds or falls short of the mean, and consequently, the degree to which the projected value matches the actual value. Additionally, the Percentage of Correctly Identified Droughts (POCID) is another critical metric. It is calculated as in Equation (8) to (14) as follows:

$$POCID = \frac{\text{Number of Correctly Identified Droughts}}{\text{Total Number of Drought Instances}} * 100 \quad (8)$$

Most of the time, the interval falls between zero and one; zero denotes no forecast, simply taking the mean, and one signifies complete accuracy of all predictions [51, 52]. The formulas are as follows:

$$RMSE = \sqrt{\frac{SSE}{N}} \quad (9)$$

SSE is the sum of squared errors, and N is the number of samples used. SSE is given by

$$SSE = \sum_{i=1}^N (y_i - \hat{y}_i)^2 \quad (10)$$

Given that the variables have already been established.

$$MAE = \frac{1}{N} \sum_{i=1}^N |(\hat{y}_i - y_i)| \quad (11)$$

The nearer the RMSE and MAE are to 0, the greater the similarity between the two samples (predictor and observation). The coefficient of determination is:

$$R^2 = \frac{\sum_{i=1}^N (y_i - \hat{y}_i)^2}{(y_i - \bar{y})^2} \quad (12)$$

$$\bar{y} = \frac{\sum_{i=1}^N y_i}{N} \quad (13)$$

$$NSE = 1 - \frac{\sum_{i=1}^N (y_i - \hat{y}_i)^2}{\sum_{i=1}^N (y_i - \bar{y})^2} \quad (14)$$

y_i is the observed value at time i ($i \in 1, \dots, N$), \bar{y} is the mean value taken over N , N is the total data size of y_i ($i \in 1, \dots, N$), and \hat{y}_i is the forecast value at time i .

3. Results and discussion

3.1 Precipitation

The average annual rainfall for the six sites is approximately 100.86 mm, with maximum and minimum temperatures recorded at 30.6 °C and 17.27 °C, respectively, throughout the period from 1991 to 2021. The trend component facilitates the identification of the data's overall behavior or tendencies, independent of seasonal trends and short-term fluctuations. The data show no significant increase or downward trend during the analyzed period, as indicated by the trend map. The trend map indicates the absence of a discernible pattern, suggesting that the data are fundamentally stable or fluctuate around a particular level. Figure 3 shows the average monthly rainfall statistics obtained during a specific period, which is from 1991 to 2021. The trend line (expressed by the Equation $y=0.3476 x$) indicates the general trend of the data. The coefficient value of 0.5752 indicates that approximately 57.52% of the variation in rainfall amounts can be explained by time, suggesting a moderately positive relationship between years and rainfall amounts. This evidence suggests that as time progresses, there is a measurable influence on rainfall trends, indicating a moderately positive relationship. Conversely, the remaining 42.48% of the variance is unexplained. This means that while time has a significant effect on rainfall, other factors are also at play that contribute to fluctuations in rainfall amounts. These factors could include climatic variations, geographical influences, or other environmental changes not directly accounted for by the time variable alone. The distribution of annual rainfall varies from year to year, as shown in Figure 4.

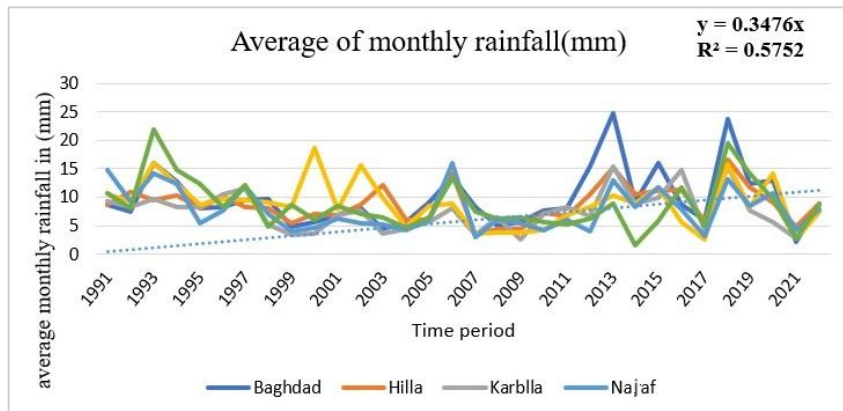


Figure 3: The average monthly rainfall quantities at several stations from 1991 to 2021

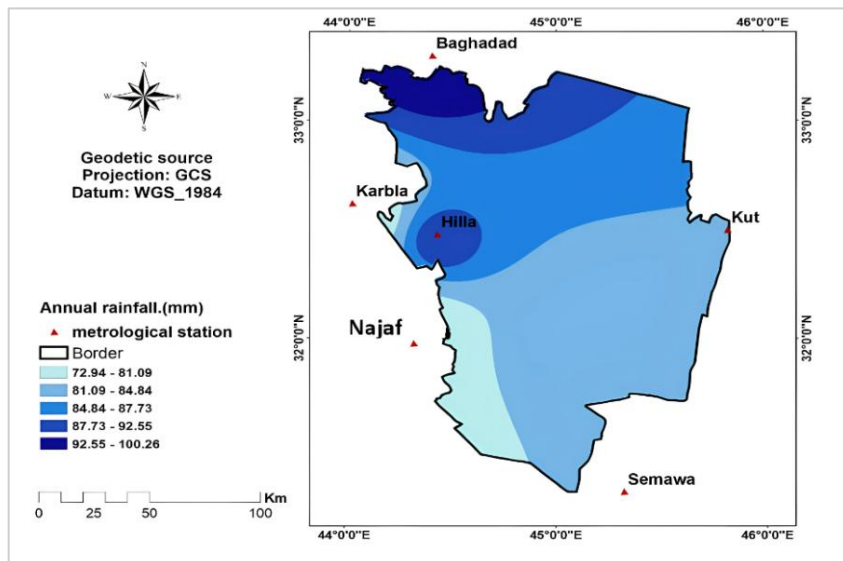


Figure 4: Distribution of annual rainfall in the study area according to the meteorological stations

3.2 Drought indices analysis by SPI and RDI

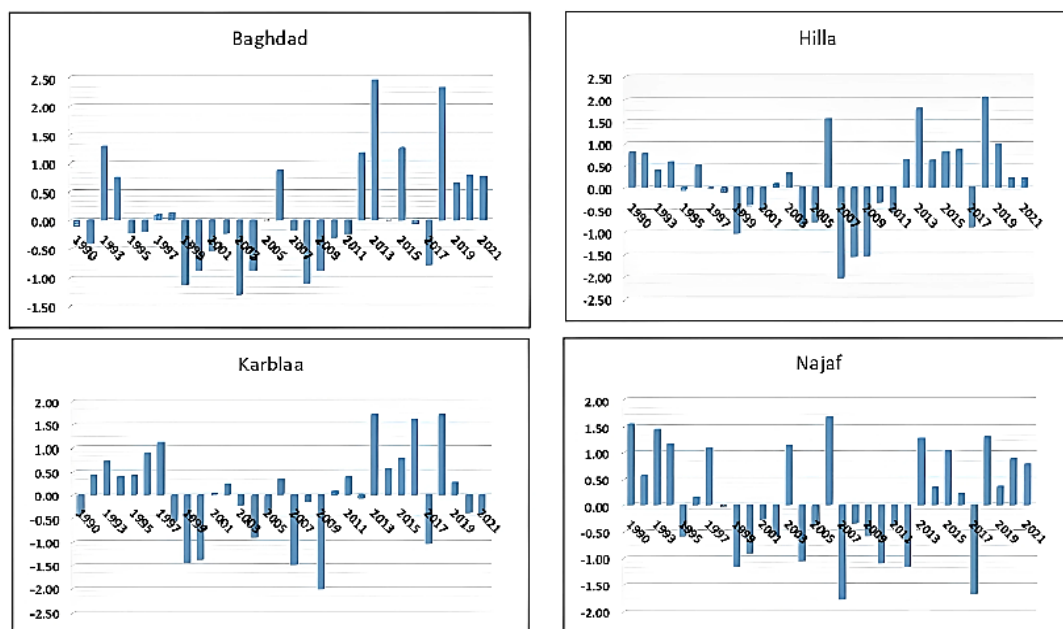
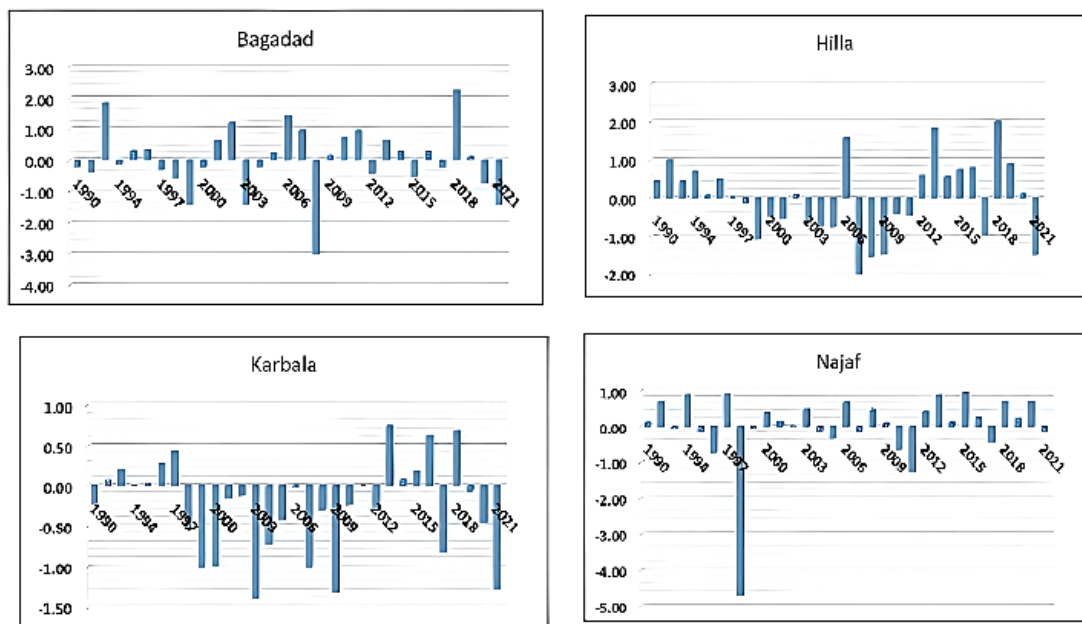
The study examines the temporal distribution of SPI values annually from 1991 to 2021. The results show that as the period increases, the frequency of dry periods increases. Severe drought conditions were observed in 2003, 2008, 2009, and 2021 in all stations, including Baghdad and Diwaniyah stations. Moderate drought was observed in 2000, 2007, 2008, 2009, 1995, 1999, 2011, 2016, and 2013. Most values were close to zero during 1991, 1992, 1994, 2005, 2010, and 2013, with humid conditions and high positive SPI values in Baghdad in 2013. The percentages of mildly drought periods increased, while extremely dry periods decreased and extremely wet periods increased, as shown in Figure 5 and Table 4. The table shows the Social Performance Index (SPI) and Relative Development Index (RDI) values from 1991 to 2021, revealing significant trends and fluctuations. The SPI initially showed strong social performance but a slight decrease to 76.3% in 1992. From 1993 to 1997, the SPI showed relatively stable values. However, a significant drop in 1998, indicating deteriorating social conditions, continued until 2005. Between 2006 and 2013, the SPI showed signs of recovery, peaking at 90.0% in 2013. The SPI's persistent decline by 2021 raises concerns about the sustainability of social improvements and population well-being. The RDI's decline from 43.0% in 1991 to -147.3% by 2021 suggests systemic issues hindering development efforts. Future research should focus on identifying factors contributing to these trends and exploring solutions for sustainable development.

Figure 6 shows the length, severity, and highest occurrence values of arid values found by RDI at all stations. However, the highest drought value of the period experienced a decrease in absolute terms. The maximum drought occurred in 1998 and 2008, specifically in the Hilla, Baghdad, and Najaf regions, where the values of RDI reached (-4.70 and -3.00), respectively. The years with moderate drought include 1991, 1992, 1994, 2003, 2004, 2015, 2016, and 2021. The RDI values in these years show that most stations experienced moderate drought. In 2013, 2014, and 2016, the values were close to zero, indicating normal or wet conditions, according to figures 5 and 6. There is a large oscillation in drought levels over the years. In certain years, regions have experienced severe drought conditions, while others have been characterized by excessive rainfall. However, recent years, particularly in 2021, have indicated a resurgence of severe drought, which poses significant risks to agriculture and water resources. This variability in drought conditions has led to both extreme drought and wet phases, adversely affecting agricultural productivity and water supply systems. Continuous monitoring of these conditions is essential for developing effective water management and agricultural policies, particularly in the context of ongoing climate change and shifting precipitation patterns.

Table 4: Social Performance Index (SPI) and Relative Development Index (RDI) with Percentage Changes Over Time

Years	SPI (%)	RDI (%)	Relative Changes (SPI) %	Relative Changes(RDI)%
1991	80.0	43.0	-	-
1992	76.4	99.3	-4.5	130.2
1993	76.4	-4.5	0.0	0.0
1994	69.7	99.3	0.0	-9.1%
1995	41.0	43.0	-48.8	0.0%
2000	-9.5	-46.7	-132.3	-108.5
2005	-76.5	-74.9	-703.1	-60.1
2010	-10.0	-74.9	87.9	0.0
2015	62.0	90.0	720.0	120.1
2021	-134.0	-147.3	-316.1	-163.7

The relative change is calculated as the percentage change from the previous year. The values in the relative change column for the first year (1991) do not have prior data; hence, the dash (-) is used.

**Figure 5:** Drought index by SPI for metrological stations from 1991 to 2021**Figure 6:** Drought index by RDI for metrological stations from 1991 to 2021

3.3 ARIMA model Test and result

This paper uses the POCID, R^2 , and RMSE to select the best model. Table 4 displays the results, including the optimal model selection and residual test results. There are noticeable variations in the amounts of rainfall that occur each year. The Drought Index (SPI-12 and RDI-12) data from different stations (Baghdad, Hala, Najaf, Diwaniyah, and Karbala) over a year are shown in Tables 4 and 5. These tables compare and contrast the data with an analytical model (ARIMA). The high POCID values showed the model's ability to identify drought periods accurately. For instance, in Baghdad, the ARIMA (1,1,1) model successfully identified 52.6% of the drought cases correctly for both indicators (RDI and SPI). Similar to the MAE values, the same model, ARIMA (1,1,1), was 0.89, which means that the forecasts were close to the actual values. The AIC criterion, which assesses the quality of various models based on the number of parameters, demonstrated this by reaching a value of 77.25, signifying a robust model with reasonable performance. According to Table 4, the R^2 of the ARIMA (6,1,1) model is 0.89, which means that the model explains 89% of the variance in the data. The RMSE of the ARIMA (1,1,1) model is 0.71, which indicates that the forecasts were relatively accurate. We tried different ARIMA models like (1,1,1) and (6,1,1) to find the best one for each station. The most suitable model for forecasting drought or rain at various stations can be found by evaluating several metrics, including POCID, R^2 , and RMSE. The tables imply that local factors like terrain and climate influence model performance by station. This information helps studies of weather trends and the management of water resources. Especially the 6-1 model, the ARIMA model demonstrated good R^2 and POCID values in both drought and rainfall, hence supporting water resource management and climate planning. The tables offer insightful analysis of ARIMA model performance under drought and rainfall, hence supporting climate planning and water resources management. As a result, the ARIMA (6,1,1) model at Hilla station proved its strength in both tables, as it recorded the highest POCID (76.3%) in both cases and recorded a high R^2 . The ARIMA (1,1,1) model shows good performance at most stations, as it obtained the best values in POCID at several stations, making it a reliable model.

Table 5: Performance measures for comparison of observed and predicted data for SPI-12 months

station	Model ARIMA(p, d, q)	POCID	R2	RMSE
Baghdad	ARIM (1,1,1)	52.6	-0.458	1.405
	ARIMA (6,1,1)	89.5	0.82	0.33
	ARIMA (6,2,0)	78.9	0.818	0.34
Hilla	ARIMA(1,1,1)	36.8	-0.57	1.438
	ARIMA (6,1,1)	94.7	0.87	0.145
	ARIMA (6,2,0)	89.5	0.94	0.48
Najaf	ARIMA(1,1,1)	47.4	-0.71	1.34
	ARIMA (6,1,1)	100	0.925	0.184
	ARIMA (6,2,0)	100	0.948	0.15
Karbala	ARIMA(1,1,1)	94.7	-0.28	1.177
	ARIMA (6,1,1)	97.7	0.85	0.215
	ARIMA (6,2,0)	94.2	0.84	0.231

3.4 ARIMA and random forest model fitting: training, testing, and forecasting

The study uses the SPI time series to analyze the annual trend of the data. The data is divided into two segments: training and testing. We allocate 80% of the data for training and 20% for testing. This paper presents a new drought prediction method based on the SPI and RDI with higher accuracy than traditional methods. By combining the advantages of the linear ARIMA model, a method was proposed to predict. SPI and RDI values for ten years are shown in Table 6. The model performs better in forecasting long-term outcomes (SPI-12 and RDI-12). We also plot the annual mean of the SPI time series to analyze the yearly trend of the data. Joint plots illustrate the relationship between observed and expected values, with a positive slope indicating a favorable correlation. The ARIMA model shows superior prediction capability at the SPI12 scale. The SPI forecast for Baghdad indicates a significant rainfall deficit, with a confidence interval ranging from -0.75 to -0.29. Both models exhibit optimal accuracy with a lead time of 1-2 months. With a confidence interval of 0.13 to 0.70. Hillah experiences a slight deficit, while Najaf shows a significant deficit, indicating a serious shortfall. These projections highlight the need for efficient water and agricultural solutions in these regions. As shown in Figure 7 (a and b), and Figure 8 (a and b), the prediction accuracy of the ARIMA model for short time scales of SPI and RDI was significantly lower than that for long time scales. In this study, performance metrics such as Root Mean Square Error (RMSE) and Adjusted R^2 were used to evaluate the effectiveness of Random Forest (RF) and ARIMA models in drought prediction. The Random Forest (RF) machine learning algorithm and the ARIMA model are compared in this study to see which one can better predict the Standard Precipitation Index (SPI) and the Reconnaissance Drought Index (RDI). We train both models on historical data and use the same training and testing datasets. This study found that the RF model correctly predicted droughts, with scores of 0.856, 0.551, and 0.218 for RDI-12 scales. Table 7 shows the Standard Precipitation Index (SPI) and Reconnaissance Drought Index (RDI) predictions for various locations using ARIMA and Random Forest models.

Table 6: Performance measures for comparison of observed and predicted data for RDI-12 months

	Model ARIMA (p, d, q)	POCID	R2	RMSE
Baghdad	ARIMA(1,1,1)	52.6	-0.078	1.176
	ARIMA (6,1,1)	68.4	0.86	0.171
	ARIMA (6,2,0)	78.9	0.818	0.34
	ARIMA(1,1,1)	36.8	-0.67	1.468
Hilla	ARIMA (6,1,1)	42.1	0.96	0.58
	ARIMA (1,2,1)	63.2	-0.76	1.506
	ARIMA (1,2,1)	52.9	-1.519	1.155
Najaf	ARIMA (6,1,1)	47.4	0.76	0.79
	ARIMA (1,1,1)	31.6	-0.25	0.60
	ARIMA(1,1,2)	52.6	-0.307	1.71
Karbala	ARIMA (6,1,1)	63.2	0.91	0.206
	ARIMA (6,2,0)	52.6	0.717	0.514
	*POCID (Percentage of Correctly Identified Droughts)			
	*RMSE (Root Mean Square Error)			
	(p, d, q)			
	P: Auto regression order d: differencing degree q : moving average order			

Table 7: Forecasting SPI and RDI for the future period (2020–2030) using the ARIMA Model

station	SPI		RDI			
	(forecast) continuous	Confidence Interval Low 59%	Confidence Interval High 59%	(forecast) continuous	Confidence Interval Low 59%	
Baghdad	-0.53	-1.35	0.29	0.22	-0.52	0.96
	-0.08	-0.92	0.76	0.14	-0.67	0.95
	-0.03	-0.87	0.81	0.09	-0.73	0.92
	-0.02	-0.86	0.82	0.07	-0.76	0.91
	-0.02	-0.86	0.82	0.06	-0.77	0.90
	-0.02	-0.86	0.82	0.06	-0.78	0.89
	-0.02	-0.86	0.82	0.05	-0.78	0.89
	-0.02	-0.86	0.82	0.05	-0.78	0.88
	-0.02	-0.86	0.82	0.05	-0.78	0.88
	-0.02	-0.86	0.82	0.05	-0.78	0.88
	-0.07	-0.91	0.78	0.42	-1.23	0.39
	-0.60	-1.58	0.37	-0.13	-0.97	0.72
Hilla	-0.44	-1.49	0.62	-0.05	-0.90	0.80
	-0.84	-2.04	0.36	-0.03	-0.88	0.82
	-0.36	-1.69	0.96	-0.02	-0.87	0.83
	-0.95	-2.37	0.48	-0.02	-0.87	0.83
	-0.49	-2.04	1.05	-0.02	-0.87	0.83
	-1.01	-2.65	0.64	-0.02	-0.87	0.83
	-0.58	-2.33	1.18	-0.02	-0.87	0.83
	-1.10	-2.95	0.75	-0.02	-0.87	0.83
	0.03	-0.78	0.84	0.02	-0.83	0.86
	0.02	-0.79	0.84	0.00	-0.85	0.84
	0.02	-0.80	0.83	0.00	-0.85	0.85
	0.02	-0.80	0.83	0.00	-0.85	0.85
Najaf	0.01	-0.81	0.83	0.00	-0.85	0.85
	0.01	-0.81	0.83	0.00	-0.85	0.85
	0.01	-0.81	0.83	0.00	-0.85	0.85
	0.01	-0.82	0.83	0.00	-0.85	0.85
	0.00	-0.82	0.83	0.00	-0.85	0.85
	0.00	-0.82	0.83	0.00	-0.85	0.85
	-0.36	-1.15	0.42	-0.45	-0.94	0.05
	-0.21	-1.00	0.59	-0.44	-0.96	0.08
	-0.13	-0.93	0.67	-0.44	-0.98	0.10
	-0.09	-0.89	0.71	-0.44	-1.00	0.12
	-0.06	-0.86	0.74	-0.44	-1.01	0.14
	-0.05	-0.85	0.75	-0.44	-1.03	0.16
Karbala	-0.05	-0.85	0.75	-0.44	-1.05	0.18
	-0.05	-0.85	0.75	-0.44	-1.07	0.19
	-0.04	-0.84	0.76	-0.44	-1.09	0.21
	-0.04	-0.84	0.76	-0.44	-1.10	0.23

The ARIMA model is more accurate for long-term projections, particularly for Najaf station, where it predicts a significant rainfall shortfall of -0.80. The Random Forest model, while effective, often underestimates deficiencies in high-stress regions. The ARIMA model has reduced confidence intervals for SPI forecasts, indicating increased dependability. The ARIMA model also has more stable predictions over extended periods, particularly in forecasting SPI values. The ARIMA model is easier to understand and predict long-term drought conditions, while the Random Forest model may lack transparency in the prediction process. The study shows how important traditional statistical models are for understanding how things change over time and how machine learning techniques can make existing methods better by finding complicated patterns. Mean square error, root mean square error, adjusted R^2 , and regression analysis were used. Machine learning models are potential drought warning techniques due to their time efficiency, fewer inputs, and less sophistication. The ARIMA model predicts a significant decrease in precipitation in Baghdad, while the RF model predicts a -0.20 SPI with a tight confidence interval. Both models have a high degree of concordance, with Hillah forecasting an SPI of -0.01. However, in Najaf, there are significant discrepancies, possibly due to the RF model's sensitivity to complex data patterns and its use of nonlinear data. Understanding these differences is crucial for understanding the precision of drought prediction models at each location. According to Xu et al. [32], the hybrid ARIMA-SVR model exhibited superior predictive accuracy compared to the standalone ARIMA model for lead times of 1–6 months and effectively modeled the SPI values using different temporal scales.

Table 8: Summarized comparison of the forecasts generated by the ARIMA and Random Forest models for SPI and RDI

station	Model	Forecast (SPI)	Confidence Interval (Low)	Confidence Interval (High)	Forecast (RDI)	Confidence Interval (Low)	Confidence Interval (High)
Baghdad	ARIMA	-0.53	-0.75	-0.29	-0.02	-0.01	0.06
	Random Forest	-0.45	-0.7	-0.2	-0.01	-0.08	0.05
Hilla	ARIMA	-0.02	0.10	0.06	-0.01	-0.09	0.07
	Random Forest	-0.01	-0.08	0.1	0.03	-0.05	0.11
Najaf	ARIMA	-0.08	-1.00	-0.06	-0.04	-0.12	0.04
	Random Forest	-0.65	-0.9	-0.45	-0.03	-0.11	0.05
Karbala	ARIMA	-0.21	-0.36	-0.06	-0.09	-0.19	0.01
	Random Forest	-0.13	-0.30	0.04	-0.06	-0.16	0.04

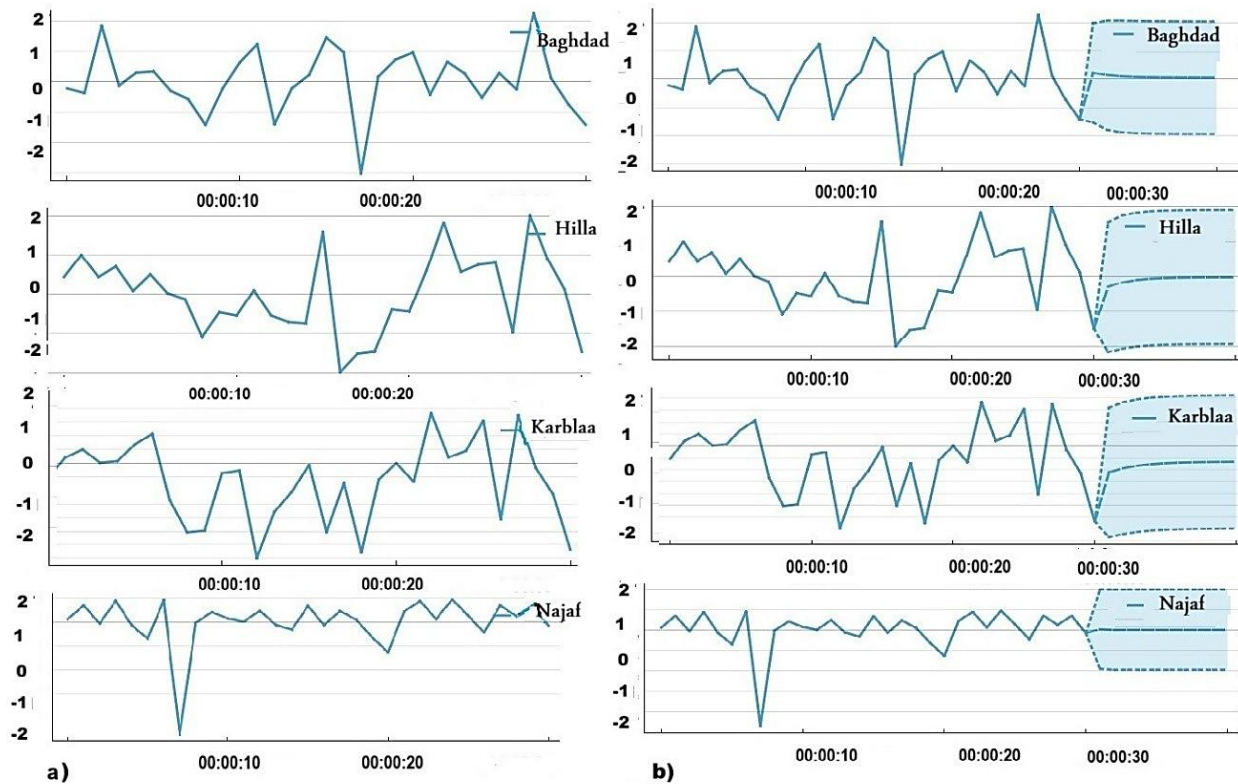


Figure 7: Forecast of multi-timescale RDI value of the meteorological stations of the ARIMA model for the period (1991-2021): a) observed RDI, b) ARIMEI-predicted RDI for ten years

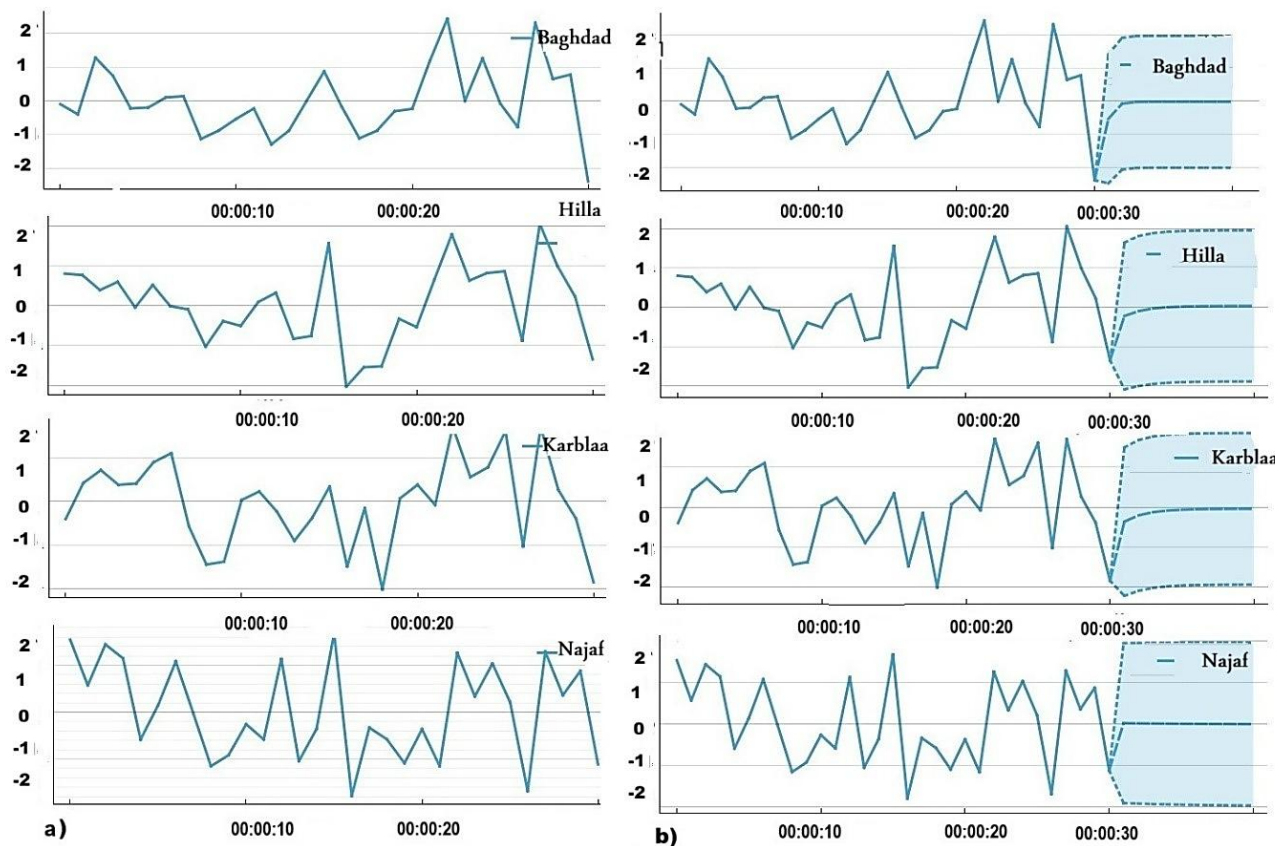


Figure 8: Forecast of multi-time-scale SPI value of the meteorological stations of the ARIMA model for the period (1991-2021): a) observed SPI, b) ARIMEI-predicted SPI for ten years

4. Conclusion

This paper emphasizes the importance of strengthening research on drought monitoring and prediction for governmental entities to prevent and reduce losses from drought disasters. It uses the SPI and RDI index and rainfall data from the national meteorological stations. According to the study, the ARIMA model achieves an R² value of 0.925 in Najaf, compared to the Random Forest (RF) model's R² of 0.551, by utilising the SPI and RDI indices in conjunction with rainfall data from national meteorological stations to provide better long-term forecasts. The study compares the ARIMA model with the Random Forest (RF) algorithm, finding that ARIMA provides more accurate long-term predictions, while RF often underestimates deficiencies in high-stress areas. The ARIMA model provides clearer insights into temporal variations and more consistent long-term forecasts, despite the time-efficient nature of RF approaches. Orange software has proven successful in predicting drought signals in conjunction with the ARIMA model. The ARIMA model also shows reduced confidence intervals, indicating increased reliability. Although RF models are time-efficient, ARIMA remains clearer in understanding temporal changes. The use of Orange software with the ARIMA model shows great effectiveness in predicting drought indicators. By combining historical data with advanced analysis tools, accurate predictions can be achieved that help address future environmental challenges. It is necessary to monitor these indicators periodically for effective water and agricultural resource management planning, especially in light of ongoing climate change.

Author contributions

Conceptualization, **Z. kadhumi**, and **A. Alhameedawi**; data curation, **Z. kadhumi**; formal analysis, **Z. kadhumi**; investigation, **Z. kadhumi** and **M. Hamoodi**; methodology, **Z. kadhumi**; project administration, **Z. kadhumi**; resources, **Z. kadhumi**; software, **Z. kadhumi**; supervision, **A. Alhameedawi**, and **M. Hamoodi**; validation, **Z. kadhumi**, **A. Alhameedawi**, and **M. Hamoodi**; visualization, **Z. kadhumi**; writing—original draft preparation, **Z. kadhumi**; writing—review and editing, **A. Alhameedawi** and **M. Hamoodi**. All authors have read and agreed to the published version of the manuscript.

Funding

This research received no specific grant from any funding agency in the public, commercial, or not-for-profit sectors.

Data availability statement

The data that support the findings of this study are available on request from the corresponding author.

Conflicts of interest

The authors declare that there is no conflict of interest.

References

- [1] T. S. Najihah, M. H. Ibrahim, N. A. M. Zain, R. Nulit, and P. E. M. Wahab, Activity of the oil palm seedlings exposed to a different rate of potassium fertilizer under water stress condition, *AIMS Environ. Sci.*, 7 (2020) 46-68. <http://dx.doi.org/10.3934/environsci.2020004>
- [2] B. S. Jasim, O. Z. Jasim, and A. N. AL-Hameedawi, A review for vegetation vulnerability using artificial intelligent (AI) techniques, *AIP Conf. Proc.*, 3092, (2024) 040002. <https://doi.org/10.1063/5.0199653>
- [3] B. S. Jasim, O. Z. Jasim, and A. N. AL-Hameedawi, Monitoring Change Detection of Vegetation Vulnerability Using Hotspots Analysis, *IIUM Eng. J.*, 25 (2024) 116-129. <https://doi.org/10.31436/ijumej.v25i2.3030>
- [4] C. Beşel and E. T. Kayıkçı, Investigation of Black Sea mean sea level variability by singular spectrum analysis, *Int. J. Eng. Geosci.*, 5 (2020) 33-41. <http://dx.doi.org/10.26833/ijeg.580510>
- [5] S. S. Ojha, V. Singh, and T. Roshni, Comparison of meteorological drought using SPI and SPEI, *Civ. Eng. J.*, 7 (2021) 2130-2149. <https://doi.org/10.28991/cej-2021-03091783>
- [6] M. H. Al-Helaly, I. A. Alwan, and A. N. Al-Hameedawi, Land covers monitoring for Bahar-Al-Najaf (Iraq) based on sentinel-2 imagery, *J. Phys. Conf. Ser.*, 1973 (2021) 12189. <https://doi.org/10.1088/1742-6596/1973/1/012189>
- [7] M. H. Al-Helaly, I. A. Alwan, and A. N. Al-Hameedawi, Assessing land cover for Bahar Al-Najaf using maximum likelihood (ML) and artificial neural network (ANN) algorithms *J. Phys. Conf. Ser.*, 1973 (2021) 12190. <https://doi.org/10.1088/1742-6596/1973/1/012190>
- [8] M. N. Hamoodi, Investigating the effects of armed and political conflicts on the land use/cover change and surface Urban Heat Islands: a case study of Baghdad, Iraq, *J. Indian Soc. Remote Sens.*, 49 (2021) 1493-1506. <https://doi.org/10.1007/s12524-021-01330-9>
- [9] S. An, G. Park, H. Jung, and D. Jang, Assessment of future drought index using SSP scenario in Rep. of Korea, *Sustainability*, 14 (2022) 4252. <https://doi.org/10.3390/su14074252>
- [10] Z. T. Abdulrazzaq, R. H. Hasan, and N. A. Aziz, Integrated TRMM Data and Standardized Precipitation Index to Monitor the Meteorological Drought, *Civ. Eng. J.*, 5 (2019) 1590-1598. <https://doi.org/10.28991/cej-2019-03091355>
- [11] Z. M. Kadhum, B. S. Jasim, and A. S. J. Al-Saedi, Improving the spectral and spatial resolution of satellite image using geomatics techniques, *AIP Conf. Proc.*, 2776 (2023) 040011. <https://doi.org/10.1063/5.0138463>
- [12] Z. A. Alemu, E. C Dioha, and M. O Dioha, Hydro-meteorological drought in Addis Ababa: A characterization study, *AIMS Environ. Sci.*, 8 (2021) 148-168. <http://dx.doi.org/10.3934/environsci.2021011>
- [13] T. A. Awchi and A. I. Jasim, Rainfall Data Analysis and Study of Meteorological Draught in Iraq for the Period 1970-2010, *Tikrit J. Eng. Sci.*, 24 (2017) 110-121. <http://dx.doi.org/10.25130/tjes.24.2017.12>
- [14] M. Fadhil, M. N. Hamoodi, and A. R. T. Ziboon, Mitigating urban heat island effects in urban environments: strategies and tools, *IOP Conf. Ser. Earth Environ. Sci.*, 1129 (2023) 012025. <https://doi.org/10.1088/1755-1315/1129/1/012025>
- [15] D. Tigkas, H. Vangelis, and G. Tsakiris, The RDI as a composite climatic index, *Eur. Water*, 41 (2013) 17-22.
- [16] T. B. McKee, N. J. Doesken, and J. Kleist, The relationship of drought frequency and duration to time scales, *Proc. 8th Conf. Appl. Climatol.*, Boston, (1993) 179-183.
- [17] H. Aksoy et al., SPI-based drought severity-duration-frequency analysis, 13th International Congress on Advances in Civil Engineering, Izmir/Turkey, 2018.
- [18] M. Naem, R. Corner, and A. Dewan, Diurnal and seasonal surface temperature variations: A case study in Baghdad, *Proceedings of the 3rd Annual Conference of Research@ Locate*, 2016, 12-14.
- [19] S. Pashiardis and S. Michaelides, Implementation of the standardized precipitation index (SPI) and the reconnaissance drought index (RDI) for regional drought assessment: a case study for Cyprus, *Eur. Water*, 23 (2008) 57-65.
- [20] H. Muhamed, M. N. Hamoodi, and A. A. T. Ziboon, Mapping and Analyzing Flood Hazard Using Remote Sensing and GIS Techniques in Diyala River Basin, Iraq, *Geotechnical Engineering and Sustainable Construction: Sustainable Geotechnical Engineering*, Springer, 2022, 759-768. http://dx.doi.org/10.1007/978-981-16-6277-5_61
- [21] S. W. Kim, D. Jung, and Y.-J. Choung, Development of a multiple linear regression model for meteorological drought index estimation based on landsat satellite imagery, *Water*, 12 (2020) 3393. <https://doi.org/10.3390/w12123393>

[22] B. S. Jasim, Z. M. K. Al-Bayati, and M. K. Obaid, Accuracy of horizontal coordinates of cadastral maps after geographic regression and their modernization using gis techniques, *Int. J. Civ. Eng. Technol.*, 9 (2018) 1395-1403.

[23] B. S. Jasim, O. Z. Jasim, and A. N. AL-Hameedawi, Evaluating land use land cover classification based on machine learning algorithms, *Eng. Technol. J.*, 42 (2024) 557-568. <http://dx.doi.org/10.30684/etj.2024.144585.1638>

[24] S. Ghosh and P. P. Mujumdar, Nonparametric methods for modeling GCM and scenario uncertainty in drought assessment, *Water Resour. Res.*, 43 (2007) W07405. <http://dx.doi.org/10.1029/2006WR005351>

[25] D. Xu, Q. Zhang, Y. Ding, and D. Zhang, Application of a hybrid ARIMA-LSTM model based on the SPEI for drought forecasting, *Environ. Sci. Pollut. Res.*, 29 (2022) 4128-4144. <https://doi.org/10.1007/s11356-021-15325-z>

[26] A. Mossad and A. A. Alazba, Drought forecasting using stochastic models in a hyper-arid climate, *Atmosphere (Basel)*, 6 (2015) 410-430. <https://doi.org/10.3390/atmos6040410>

[27] M. Seibert, B. Merz, and H. Apel, Seasonal forecasting of hydrological drought in the Limpopo Basin: a comparison of statistical methods, *Hydrol. Earth Syst. Sci.*, 21 (2017) 1611-1629. <https://doi.org/10.5194/hess-21-1611-2017>

[28] I. A. Alwan, N. A. Aziz, and M. N. Hamoodi, Potential water harvesting sites identification using spatial multi-criteria evaluation in Maysan Province, Iraq, *ISPRS Int. J. Geo-Information*, 9 (2020) 1611-1629. <https://doi.org/10.5194/hess-21-1611-2017>

[29] K. F. Fung, Y. F. Huang, C. H. Koo, and M. Mirzaei, Improved SVR machine learning models for agricultural drought prediction at downstream of Langat River Basin, Malaysia, *J. Water Clim. Chang.*, 11 (2020) 1383-1398. <https://doi.org/10.2166/wcc.2019.295>

[30] A. N. M. Al-Hameedawi, Fuzzy logic approach based on geomatics and remote sensing for siting a petroleum warehouse in the metropolitan area of Baghdad, *J. Indian Soc. Remote Sens.*, 50 (2022) 1211-1225. <https://doi.org/10.1007/s12524-022-01517-8>

[31] V. Poonia, Estimation of Standardized Precipitation Evapotranspiration Index (SPEI) and drought modeling using ARIMA time series in Raichur , pp. 1–22, 2024.

[32] D. Xu, Q. Zhang, Y. Ding, and H. Huang, Application of a hybrid arima–svr model based on the spi for the forecast of drought—A case study in Henan province, China, *J. Appl. Meteorol. Climatol.*, 59 (2020) 1239-1259. <https://doi.org/10.1175/JAMC-D-19-0270.1>

[33] Z. M. Kadhum, B. S. Jasim, and M. K. Obaid, Change detection in city of Hilla during period of 2007-2015 using Remote Sensing Techniques, *IOP Conf. Ser. Mater. Sci. Eng.*, 737 (2020) 12228. <https://doi.org/10.1088/1757-899X/737/1/012228>

[34] A. S. J. Al-Saedi, Z. M. Kadhum, and B. S. Jasim, Land use and land cover analysis using geomatics techniques in Amara City, *Ecol. Eng.*, 9 (2023) 161-169. <https://doi.org/10.12912/27197050/173211>

[35] F. A. O. AQUASTAT, Transboundary River Basins—Euphrates-Tigris River Basin, Rome Food Agric. Organ. United Nations, 2009.

[36] B. S. Jasim, O. Z. Jasim, and A. N. Al-hameedawi, Calculation Soil Moisture Index (SMI) from Landsat- 5 Thematic Mapper (TM) Satellite Images, *AIP Conf. Proc.*, 3219 (2024) 020118. <https://doi.org/10.1063/5.0236187>

[37] D. Tigkas, H. Vangelis, and G. Tsakiris, DrinC: a software for drought analysis based on drought indices, *Earth Sci. Informatics*, 8 (2015) 697-709. <https://doi.org/10.1007/s12145-014-0178-y>

[38] J. Demšar, T. Curk, A. Erjavec, C. Gorup, T. Hočevar., et al., Orange: data mining toolbox in Python, *J. Mach. Learn. Res.*, 14 (2013) 2349-2353.

[39] D. R. Mohanta, J. Soren, S. K. Sarangi, and S. Sahu, Meteorological drought trend analysis by standardized precipitation index (SPI) and reconnaissance drought index (RDI): a case study of Gajapati District, *Int. J. Chem. Stud.*, 8 (2020) 1741-1746. <https://doi.org/10.22271/chemi.2020.v8.i3x.9448>

[40] M. A. A. Zarch, B. Sivakumar, and A. Sharma, Droughts in a warming climate: A global assessment of Standardized precipitation index (SPI) and Reconnaissance drought index (RDI), *J. Hydrol.*, 526 (2015) 183-195. <https://doi.org/10.1016/j.jhydrol.2014.09.071>

[41] C. Cacciamani, A. Morgillo, S. Marchesi, and V. Pavan, Monitoring and forecasting drought on a regional scale: Emilia-Romagna region, *Methods tools drought Anal. Manag.*, (2007) 29-48.

[42] G. Tsakiris and D. Pangalou, Drought characterisation in the Mediterranean, *Coping with Drought Risk in Agriculture and Water Supply Systems: Drought Management and Policy Development in the Mediterranean*, Springer, (2009) 69-80. https://doi.org/10.1007/978-1-4020-9045-5_6

[43] N. Beden, V. Demir, and A. Ü. Keskin, Samsun ilinde SPI ve PNI kuraklık indekslerinin eğilim analizi, Dokuz Eylül Üniversitesi Mühendislik Fakültesi Fen ve Mühendislik Derg., 22 (2020) 107-116. <https://doi.org/10.21205/deufmd.2020226411>

[44] M. Fadhil, A. A. T. Ziboon, and M. N. Hamoodi, Estimate near-surface temperatures based on land surface temperature: A case study of Al-Kut, Iraq, AIP Conf. Proc., AIP Publishing, 2775 (2023) 030012. <https://doi.org/10.1063/5.0141144>

[45] K. F. Fung, Y. F. Huang, C. H. Koo, and Y. W. Soh, Drought forecasting: A review of modelling approaches 2007–2017, J. Water Clim. Chang., 11 (2020) 771-799. <https://doi.org/10.2166/wcc.2019.236>

[46] Y. Zhang, H. Yang, H. Cui, and Q. Chen, Comparison of the ability of ARIMA, WNN and SVM models for drought forecasting in the Sanjiang Plain, China, Nat. Resour. Res., 29 (2020) 1447-1464. <http://dx.doi.org/10.1007/s11053-019-09512-6>

[47] S. Mehdizadeh, F. Ahmadi, A. D. Mehr, and M. J. S. Safari, Drought modeling using classic time series and hybrid wavelet-gene expression programming models, J. Hydrol., 587 (2020) 125017. <https://doi.org/10.1016/j.jhydrol.2020.125017>

[48] A. Mokhtar, M. Jajlai, H. He, N. Al-Ansari, *et al.*, Estimation of SPEI meteorological drought using machine learning algorithms, IEEE Access, 9 (2021) 65503-65523. <https://doi.org/10.1109/ACCESS.2021.3074305>

[49] Breiman, L. Random Forests. Machine Learning 45, 5–32 (2001). <https://doi.org/10.1023/A:1010933404324>

[50] T. H. Shihab, A. N. Al-Hameedawi, and A. M. Hamza, Random forest (RF) and artificial neural network (ANN) algorithms for LULC mapping, Eng. Technol. J., 38 (2020) 510-514. <https://doi.org/10.30684/etj.v38i4A.399>

[51] A. Belayneh, J. Adamowski, B. Khalil, and J. Quilty, Coupling machine learning methods with wavelet transforms and the bootstrap and boosting ensemble approaches for drought prediction, Atmos. Res., 172 (2016) 37-47. <https://doi.org/10.1016/j.atmosres.2015.12.017>

[52] R. C. Deo and M. Şahin, An extreme learning machine model for the simulation of monthly mean streamflow water level in eastern Queensland, Environ. Monit. Assess., 188 (2016) 1-24. <https://doi.org/10.1007/s10661-016-5094-9>